Mechanism of inverted-chirp infrasonic radiation from sprites

Sebastien de Larquier[1,2] and Victor P. Pasko[1]

Received 30 August 2010; revised 29 September 2010; accepted 4 October 2010; published 18 December 2010.

[1] Farges and Blanc (2010) reported inverted-chirp infrasonic signals with high frequencies arriving before low frequencies, possibly emitted by sprite discharges and observed on the ground at close range (<100 km) from the source. In the present work a parallel version of a 2-D FDTD model of infrasound propagation in a realistic atmosphere is applied to demonstrate that the observed morphology of infrasound signals is consistent with general scaling of diameters of sprite streamers inversely proportionally to the air density. The smaller structures at lower altitudes radiate higher infrasonic frequencies that arrive first at the observational point on the ground, while the low frequency components are delayed because they originate at lower air densities at higher altitudes. The results demonstrate that strong absorption of high frequency infrasonic components at high altitudes (i.e., ~0.2 dB/km for 8 Hz at 70 km) may also contribute to formation of inverted-chirp signals observed on the ground at close range. **Citation:** de Larquier, S., and V. P. Pasko (2010), Mechanism of inverted-chirp infrasonic radiation from sprites, *Geophys. Res. Lett.*, *37*, L24803, doi:10.1029/2010GL045304.

1. Introduction

[2] Atmospheric infrasonic waves are acoustic waves with frequencies ranging from 0.02 to 10 Hz [e.g., *Blanc*, 1985]. Atmospheric infrasound is generated by a variety of sources, including volcanoes, tornadoes, earthquakes [e.g., *Bedard and Georges*, 2000], lightning [e.g., *Assink et al.*, 2008], and pulsating auroras [e.g., *Wilson et al.*, 2005]. The importance of infrasound studies has been emphasized in the past ten years from the Comprehensive Nuclear Test Ban Treaty (CTBT) verification perspective [e.g., *Le Pichon et al.*, 2009]. Infrasonic signals carry important information about their sources and correct modeling interpretation of observations therefore represents an important task for better understanding of dynamical features and energetics of infrasonic wave sources.

[3] Sprites are short lasting (a few ms) luminous discharges appearing in the altitude range ~40–90 km above thunderstorms [e.g., *Pasko*, 2007, and references therein]. Recent telescopic imaging of sprites revealed fine structures in these events with transverse spatial scales ranging from a few tens of meters at lower altitudes, up to a few hundreds of meters at higher altitudes [*Gerken and Inan*, 2002].

[4] The possibility of infrasound generation by sprite discharges has been discussed by *Bedard et al.* [1999]. Specific chirp-like infrasound signatures possibly related to sprite discharges have been identified by *Liszka* [2004], and their phenomenology further discussed by *Liszka and Hobara* [2006]. *Farges et al.* [2005] reported the first unambiguous infrasound signals generated by sprites from simultaneous observations of infrasound and sprites. Observations reveal that sprites produce chirp-like infrasonic signatures, with low frequencies arriving before high frequencies when observed at a distance of ~400 km.

[5] More recently, *Farges and Blanc* [2010] reported observations of close range infrasonic signatures that could be correlated with sprite events. Those events are manifested by arrival of high frequencies before low frequencies (i.e., inverted chirps) in infrasonic signals observed within a 100 km distance from a thunderstorm known to produce sprites. Although no direct video captures of sprites can be related to the infrasound signals because the sprites where out of the camera field of view, inverse ray-tracing suggests high altitude sources between 40 and 90 km, which correspond to typical altitudes of sprites. Furthermore, the lightning activity during time periods when the infrasound signatures were observed is typical of sprite producing storms and some sprites were indeed observed but no infrasonic signal could be related to these events, most likely because the sprites in the captured subset were too small and weak. The measured signals typically have a duration of 1 min and an amplitude between 10^{-2}–10^{-1} Pa.

[6] The analysis of total energy budget associated with sprite and causative lightning discharges indicates that the observed infrasonic signatures are most likely produced by direct Ohmic heating of air in sprite columns due to a passage of electric current [*Pasko and Snively*, 2007]. The estimated heating levels in sprite streamers are expected to be small, with temperature changes $\Delta T/T \sim 0.2$–2% [*Pasko et al.*, 1998]. These estimates are consistent with an accurate analysis of energy budget of sprites by other authors indicating $\Delta T \leq 0.5$ K [*Sentman et al.*, 2003], and information on sprite rotational temperature indicating consistency of observed molecular nitrogen band emissions with rotational temperatures in the range 220–230 K (not exceeding 300 K) [*Green et al.*, 1996; *Morrill et al.*, 1998; *Bucsela et al.*, 2003; *Kanmae et al.*, 2007]. The sprite heating being instantaneous it can be assumed that pressure perturbation directly relates to temperature perturbation and a 1°K increase in temperature at 70 km altitude would translate in a 0.032 Pa. Accounting for the scaling of pressure perturbation with radial distance for a cylindrical radiator with 100 m transverse extent, the pressure perturbation expected on the ground at 60 km horizontal distance from the source would be 0.12 Pa, which matches observations by *Farges and Blanc* [2010].

[1]CSSL, Pennsylvania State University, University Park, Pennsylvania, USA.
[2]Now at SuperDARN Hf Radar Group, Virginia Polytechnic Institute and State University, Blacksburg, Virginia, USA.

0094-8276/10/2010GL045304

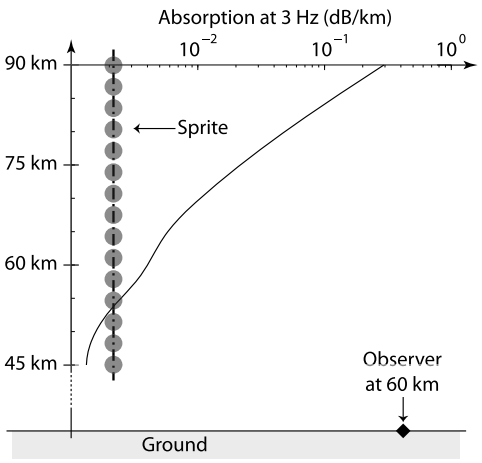

Figure 1. Cross-sectional view of the sprite in the model domain illustrating the parameters and geometry of the domain. This figure also includes the absorption coefficient adapted from *Sutherland and Bass* [2004] for a 3 Hz infrasonic wave propagating between 45 km and 90 km altitude.

[7] The goal of the present paper is to undertake FDTD modeling of inverted-chirp infrasound signals from sprites observed at close range (<100 km) and propose a specific mechanism explaining their occurrence.

2. Model Formulation

[8] The model employed in the present study utilizes linearized equations of acoustics with classical viscosity and atmospheric gravitational stratification effects to solve for perturbation in density, pressure and velocity [e.g., *Pasko*, 2009]. The attenuation of infrasonic waves in a realistic atmosphere is described using a model of *Sutherland and Bass* [2004] and is implemented in the model equations using a decomposition technique summarized by *de Groot-Hedlin* [2008], *de Larquier et al.* [2010], and *de Larquier* [2010].

[9] The model equations are implemented in a two-dimensional (2-D) axisymmetric simulation domain using a second order in time and space FDTD scheme [*de Larquier et al.*, 2010]. A parallel version of the 2-D model is implemented using a domain decomposition strategy allowing for higher computational speed and more importantly memory distribution [e.g., *Gropp et al.*, 1999]. The left boundary of the simulation domain is the axis of cylindrical symmetry, and the ground is represented as a hard perfectly reflecting boundary [e.g, *Sparrow and Raspet*, 1991]. The top and right boundaries support outgoing waves with no reflections using a nearly perfectly matched layer (NPML) similar to the one introduced in electromagnetics [*Cummer*, 2003].

[10] Results from *Farges and Blanc* [2010] suggest that the infrasound signal is strongly related to the sprite vertical extent. Remembering that the absorption increases with altitude and is proportional to the square of frequency [e.g., *Sutherland and Bass*, 2004; *de Groot-Hedlin*, 2008], it can be hypothesized that absorption scaling through the sprite vertical extent is at least partly responsible for the observed infrasonic signal. Specifically, we expect that the signal arriving from higher altitudes would naturally have a depleted high frequency content. Also, geometrical considerations indicate that such a signal would arrive to an observer positioned several tens of kilometers horizontal distance from the sprite with some delay with respect to the signal emitted from the lower portions of the sprite.

[11] Additionally, observations of *Gerken and Inan* [2003] and streamer simulation results [e.g., *Liu and Pasko*, 2004] show that streamers radii increase with altitude. Overall trend of streamers scaling is expected to proceed inversely proportionally to ambient neutral density in the atmosphere [e.g., *Liu and Pasko*, 2004]. This alone would lead to a factor of 600 wider streamers at 90 km in comparison with streamers at 45 km. Streamers in sprites, however, accelerate, expand and branch and particular diameters realized at specific altitudes depend on geometry of applied reduced electric field and history of sprite initiation and development [*Liu et al.*, 2009]. Based on observational evidence [e.g., *Gerken and Inan*, 2003] it can be assumed for quantitative estimates that low altitude streamers in sprites would have

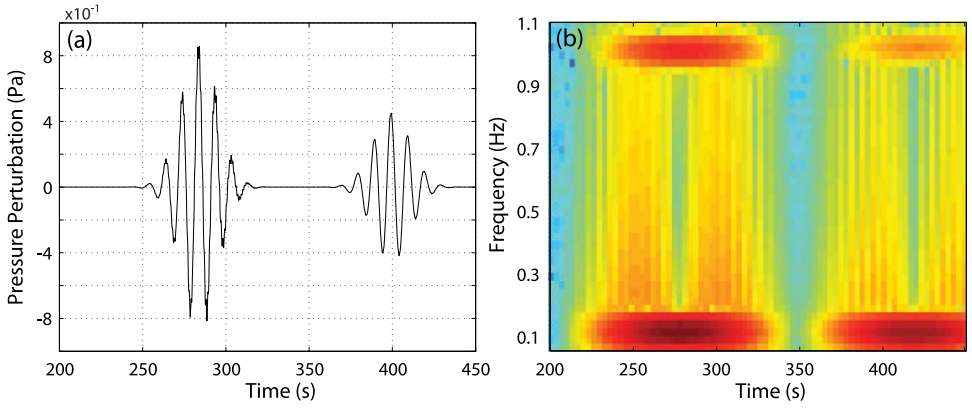

Figure 2. Modeling results for two isotropic sources (both radiating frequencies 0.1 Hz and 1 Hz) positioned at 45 km and 90 km altitudes in an atmosphere with an absorption artificially increased by a factor of 25 with respect to its standard value. (a) Pressure perturbation signal observed on the ground at 60 km horizontal distance. (b) Spectrogram of the observed signal.

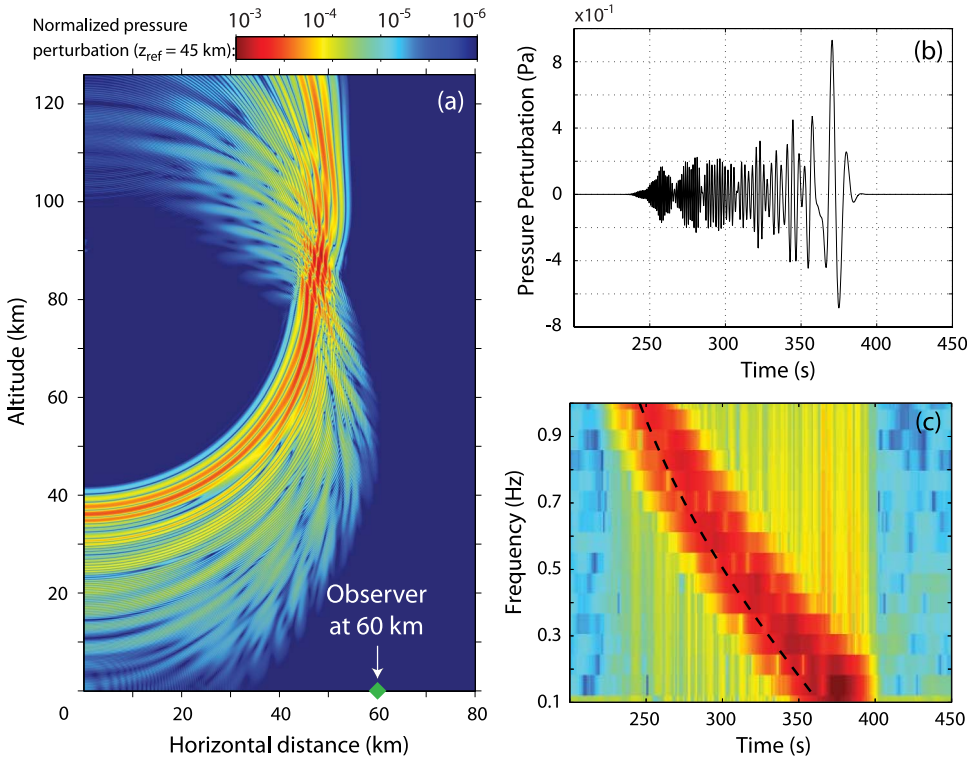

Figure 3. Modeling results for a sprite consisting of 15 isotropic sources radiating frequencies linearly varying from 0.1 Hz at 45 km altitude up to 0.9 Hz at 90 km altitude. (a) Snapshot of the normalized pressure perturbation at t = 200 s. (b) Pressure perturbation signal observed on the ground at 60 km horizontal distance. (c) Spectrogram of the observed signal (the dashed line represents the expected shape when accounting for direct propagation).

diameters d_s of 10 to 50 m, while high altitude streamers may have diameters exceeding 200 m. Combined with speeds of sound c_s of ~320 m/s and ~280 m/s at ~45 km and ~90 km altitudes, respectively [*Sutherland and Bass*, 2004], this suggests dominant infrasonic frequencies $f \simeq c_s/d_s$ of ≥8 Hz for the lower part of the sprite and ≤1 Hz for the upper part of the sprite, assuming that pressure perturbation in streamer columns (i.e., due to heating) forms on time scales $\tau_s \ll d_s/c_s$.

[12] A simplified model geometry that would approximately reproduce infrasound generation from a sprite based on altitude scalings discussed above is shown in Figure 1. A sprite is represented by a series of isotropic sources, each radiating a specific frequency content that varies from high to low frequencies with increase in altitude. The sources operate to generate pressure waves for a given time duration effectively corresponding to the travel time of an infrasonic wave through the horizontal width of the sprite. The configuration of the sources therefore allows to effectively reproduce effects of vertical and horizontal extent of the sprite.

3. Results

[13] The effect of the altitude scaling of absorption on the frequency content of the sprite is first illustrated. In order to accelerate computations, the present study employs a model set up with vertical and horizontal grid resolution of 20 m, allowing to accurately model frequencies $f \leq 1$ Hz. The absorption is artificially increased so that the maximum frequency represented (1 Hz) is attenuated as much as a frequency of 5 Hz would be attenuated under standard atmospheric conditions. The multiplication factor of the absorption coefficient is determined using the quadratic dependency of absorption on frequency [e.g., *Sutherland and Bass*, 2004], which yields a factor of 25. Figure 2 shows the results from the modeling of two sources positioned at altitudes 45 and 90 km each radiating both 0.1 Hz and 1 Hz equal magnitude signals.

[14] We next illustrate the effect of the sprite frequency content assuming the frequency range 0.1–0.9 Hz. The effects of absorption are not included in this part. Each one of the 15 sources composing the modeled sprite is assumed to radiate for 40 s to account for the large number of streamers within the horizontal extent of the sprite (i.e., this artificial duration of the radiation effectively represent a sprite with 12 km transverse extent assuming c_s ~ 300 m/s). The frequency distribution is set to vary linearly with altitude, from high to low frequencies. Figure 3a provides a 2-D snapshot of the normalized pressure perturbation $\tilde{p}/p_0(z)\sqrt{p_0(z)/p_0(z_{\mathrm{ref}})}$ at time t = 200 s, where $\tilde{p}$ is the pressure perturbation and $p_0(z)$ is the ambient profile of pressure as a function of altitude z and z_{ref} = 45 km. The related observed pressure perturbation at 60 km horizontal distance, as well as the corresponding spectrogram of the signal are presented in Figures 3b and 3c. The same simulation is repeated using a second and fourth order variation of frequency as a function of altitude such as $f = (0.1 - 0.9)(z - 45)^n/45^n + 0.9$ for 45 km ≤ z ≤ 90 km, where z is the altitude in km and n is the order of the frequency variation. The dynamic spectrograms

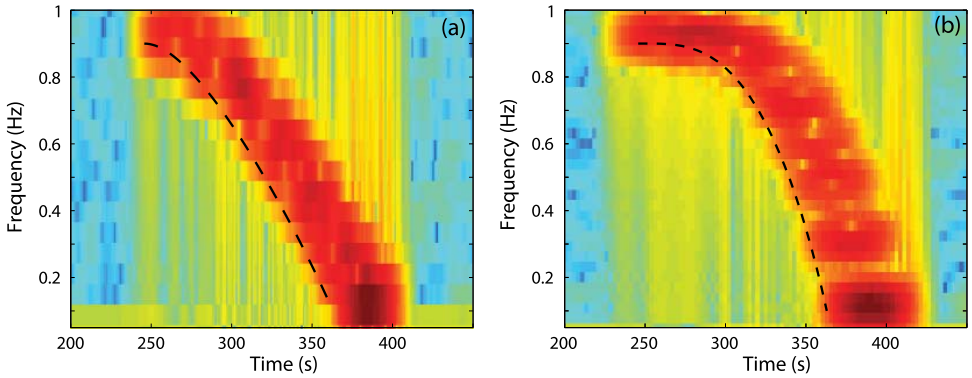

Figure 4. (a and b) Same as in Figure 3c only for sources with radiated frequencies varying as a second and fourth order function of altitude, respectively, from 0.9 Hz at 45 km to 0.1 Hz at 90 km.

of the observed pressure perturbation at 60 km horizontal distance are presented in Figures 4a and 4b.

4. Discussion

[15] It has been mentioned previously that modeling results [*Liu and Pasko*, 2004] suggest streamer radius of a few tens of meters at 70 km altitude. Given a speed of sound of ~290 m/s at this altitude, it is expected that frequencies up to 8 Hz would be generated. However, the absorption of an 8 Hz acoustic wave at 70 km altitude is ~0.2 dB/km [e.g., *Sutherland and Bass*, 2004], suggesting that such a wave would be mostly absorbed before reaching the ground. Figure 2 evidences that the high frequencies generated at high altitudes are mostly absorbed and consequently not observed on the ground. The first signal received between ~250–330 s is generated by the lower source at 45 km altitude and the second signal is generated by the upper source at 90 km. Figure 2b clearly shows that the second signal is mostly depleted of its high frequency content. As a result, the high frequencies generated in the upper part of the sprite are most likely to dissipate before reaching the ground. This effect, leading to arrival of only low frequencies at the end of the sprite generated waveform may contribute to the formation of inverted-chirp signals observed on the ground at close range [*Farges and Blanc*, 2010].

[16] The scaling of transverse dimension of streamers with altitude is expected to be a factor responsible for the frequency content of the sprite and consequently the observed inverted chirp. Results presented in Figure 3c show a linear inverted chirp on the dynamic spectrogram effectively mapping the altitude frequency distribution in the modeled sprite. It should be noted that while the frequency content and time extent of the inverted chirp are not exactly those observed by *Farges and Blanc* [2010], the results still demonstrate the effect of the propagation and observation of infrasound from a source with the same qualitative dynamics as a sprite. Specifically, the duration of the chirp signal reported in Figure 3c exceeds that reported experimentally (~1 min). This can be directly attributed to smaller vertical and horizontal extensions of sprite in experimental situation as compared to the parameters used in modeling.

[17] The shape of the inverted-chirp in Figure 3c is directly correlated with the linear frequency distribution through the sprite vertical extent. To demonstrate this relation, the modeled sprite used in Figure 3 is modified using two different altitude frequency distributions in which the frequency drops as a second and fourth order functions of altitude. Figure 4 shows that the dynamic spectrum of the pressure perturbation observed on the ground again maps well the frequency distribution as a function of altitude in the modeled sprite. This result shows that infrasound observed at close range from sprites can be used to remote sense predominant physical dimensions of radiators (i.e., streamers) in sprites responsible for infrasonic emissions.

[18] Modeling results presented in this work suggest that in specific experiments both the scaling of absorption with frequency and altitude, and the scaling of transverse dimension of filamentary structures (streamers) in sprites as a function of altitude may contribute to the observed inverted-chirp signal.

[19] The scaling of absorption in the atmosphere has also been suggested to be responsible for the chirp signals observed at long range from sprites (~400 km). *Farges et al.* [2005] proposed that the infrasound signal coming from the nearest side of the sprite (relatively to the observer) reflects at higher altitude, has reduced high-frequency content due to strong absorption at high altitudes, and arrives first at the observation point. The infrasound signal generated from the farthest side of the sprite reflects at lower altitude, has enhanced high-frequency content, and arrives second at the observation point. Ray tracing results obtained with HARPA [e.g., *Jones*, 1996] confirm the results presented by *Farges et al.* [2005], showing that the waves following a ground-thermosphere-ground path were responsible for the strongest infrasound arrival at 400 km from the sprite. Preliminary FDTD results [*de Larquier*, 2010] show an additional signal of similar amplitude generated by a thermosphere-ground path. This signal precedes the ground-thermosphere-ground signal by ~300 s. Those additional signatures have not yet been detected in experiments (T. Farges, private communication, 2010).

[20] **Acknowledgments.** This research was supported by NSF AGS-0836391 to Penn State University.

References

Assink, J. D., L. G. Evers, I. Holleman, and H. Paulssen (2008), Characterization of infrasound from lightning, *Geophys. Res. Lett.*, *35*, L15802, doi:10.1029/2008GL034193.

Bedard, A. J., and T. M. Georges (2000), Atmospheric infrasound, *Phys. Today*, *53*(3), 32–37.

Bedard, A. J., W. A. Lyons, R. A. Armstrong, T. E. Nelson, B. Hill, and S. Gallagher (1999), A search for low-frequency atmospheric acoustic waves associated with sprites, blue jets, elves, and storm electrical activity, *Eos Trans. AGU*, *80*(46), Fall Meet. Suppl., Abstract A51B-18.

Blanc, E. (1985), Observations in the upper-atmosphere of infrasonic waves from natural or artificial sources—A summary, *Ann. Geophys.*, *3*(6), 673–687.

Bucsela, E., J. Morrill, M. Heavner, C. Siefring, S. Berg, D. Hampton, D. Moudry, E. Wescott, and D. Sentman (2003), $N_2(B^3\Pi_g)$ and $N_2^+(A^2\Pi_u)$ vibrational distributions observed in sprites, *J. Atmos. Sol. Terr. Phys.*, *65*, 583–590.

Cummer, S. A. (2003), A simple, nearly perfectly matched layer for general electromagnetic media, *IEEE Microw. Wirel. Compon. Lett.*, *13*(3), 128–130.

de Groot-Hedlin, C. (2008), Finite-difference time-domain synthesis of infrasound propagation through an absorbing atmosphere, *J. Acoust. Soc. Am.*, *124*(3), 1430–1441.

de Larquier, S. (2010), Finite-difference time-domain modeling of infrasound propagation in a realistic atmosphere, M.S. thesis, Pa. State Univ., University Park.

de Larquier, S., V. P. Pasko, H. C. Stenbaek-Nielsen, C. R. Wilson, and J. V. Olson (2010), Finite-difference time-domain modeling of infrasound from pulsating auroras and comparison with recent observations, *Geophys. Res. Lett.*, *37*, L06804, doi:10.1029/2009GL042124.

Farges, T., and E. Blanc (2010), Characteristics of infrasound from lightning and sprites near thunderstorm areas, *J. Geophys. Res.*, *115*, A00E31, doi:10.1029/2009JA014700.

Farges, T., E. Blanc, A. Le Pichon, T. Neubert, and T. H. Allin (2005), Identification of infrasound produced by sprites during the Sprite2003 campaign, *Geophys. Res. Lett.*, *32*, L01813, doi:10.1029/2004GL021212.

Gerken, E. A., and U. S. Inan (2002), A survey of streamer and diffuse glow dynamics observed in sprites using telescopic imagery, *J. Geophys. Res.*, *107*(A11), 1344, doi:10.1029/2002JA009248.

Gerken, E. A., and U. S. Inan (2003), Observations of decameter-scale morphologies in sprites, *J. Atmos. Sol. Terr. Phys.*, *65*(5), 567–572.

Green, B. D., M. E. Fraser, W. T. Rawlins, L. Jeong, W. A. M. Blumberg, S. B. Mende, G. R. Swenson, D. L. Hampton, E. M. Wescott, and D. D. Sentman (1996), Molecular excitation in sprites, *Geophys. Res. Lett.*, *23*, 2161–2164.

Gropp, W., E. Lusk, and A. Skjellum (1999), *Using MPI: Portable Parallel Programming With the Message-Passing Interface*, MIT Press, Cambridge, Mass.

Jones, R. M. (1996), Three dimensional ray tracing in the atmosphere, in *The Upper Atmosphere*, edited by W. Dieminger, G. Hartmann, and R. Leitinger, pp. 307–327, Springer, Berlin.

Kanmae, T., H. C. Stenbaek-Nielsen, and M. G. McHarg (2007), Altitude resolved sprite spectra with 3 ms temporal resolution, *Geophys. Res. Lett.*, *34*, L07810, doi:10.1029/2006GL028608.

Le Pichon, A., J. Vergoz, E. Blanc, J. Guilbert, L. Ceranna, L. Evers, and N. Brachet (2009), Assessing the performance of the International Monitoring System's infrasound network: Geographical coverage and temporal variabilities, *J. Geophys. Res.*, *114*, D08112, doi:10.1029/2008JD010907.

Liszka, L. (2004), On the possible infrasound generation by sprites, *J. Low Freq. Noise Vib. Act. Control*, *23*(2), 85–93.

Liszka, L., and Y. Hobara (2006), Sprite-attributed infrasonic chirps—Their detection, occurrence and properties between 1994 and 2004, *J. Atmos. Sol. Terr. Phys.*, *68*(11), 1179–1188.

Liu, N., and V. P. Pasko (2004), Effects of photoionization on propagation and branching of positive and negative streamers in sprites, *J. Geophys. Res.*, *109*, A04301, doi:10.1029/2003JA010064.

Liu, N. Y., V. P. Pasko, K. Adams, H. C. Stenbaek-Nielsen, and M. G. McHarg (2009), Comparison of acceleration, expansion, and brightness of sprite streamers obtained from modeling and high-speed video observations, *J. Geophys. Res.*, *114*, A00E03, doi:10.1029/2008JA013720.

Morrill, J. S., E. J. Bucsela, V. P. Pasko, S. L. Berg, W. M. Benesch, E. M. Wescott, and M. J. Heavner (1998), Time resolved N_2 triplet state vibrational populations and emissions associated with red sprites, *J. Atmos. Sol. Terr. Phys.*, *60*, 811–829.

Pasko, V. P. (2007), Red sprite discharges in the atmosphere at high altitude: The molecular physics and the similarity with laboratory discharges, *Plasma Sources Sci. Technol.*, *16*, S13–S29.

Pasko, V. P. (2009), Mechanism of lightning-associated infrasonic pulses from thunderclouds, *J. Geophys. Res.*, *114*, D08205, doi:10.1029/2008JD011145.

Pasko, V. P., and J. B. Snively (2007), Mechanism of infrasound radiation from sprites, *Eos Trans. AGU*, *88*(52), Fall Meet. Suppl., Abstract AE23A-0899.

Pasko, V. P., U. S. Inan, and T. F. Bell (1998), Spatial structure of sprites, *Geophys. Res. Lett.*, *25*, 2123–2126.

Sentman, D. D., E. M. Wescott, R. H. Picard, J. R. Winick, H. C. Stenbaek-Nielsen, E. M. Dewan, D. R. Moudry, F. T. São Sabbas, M. J. Heavner, and J. Morrill (2003), Simultaneous observations of mesospheric gravity waves and sprites generated by a midwestern thunderstorm, *J. Atmos. Sol. Terr. Phys.*, *65*, 537–550.

Sparrow, V. W., and R. Raspet (1991), A numerical-method for general finite-amplitude wave-propagation in 2 dimensions and its application to spark pulses, *J. Acoust. Soc. Am.*, *90*(5), 2683–2691.

Sutherland, L. C., and H. E. Bass (2004), Atmospheric absorption in the atmosphere up to 160 km, *J. Acoust. Soc. Am.*, *115*(3), 1012–1032.

Wilson, C. R., J. V. Olson, and H. C. Stenbaek-Nielsen (2005), High trace-velocity infrasound from pulsating auroras at Fairbanks, Alaska, *Geophys. Res. Lett.*, *32*, L14810, doi:10.1029/2005GL023188.

S. de Larquier, SuperDARN Hf Radar Group, Virginia Polytechnic Institute and State University, 1991 Kraft Dr., Ste. 2019, Blacksburg, VA 24061, USA.

V. P. Pasko, CSSL, Pennsylvania State University, 227 Electrical Engineering East, University Park, PA 16802, USA. (vpasko@psu.edu)